

Dechuck Operation of Coulomb Type and Johnsen-Rahbek Type of Electrostatic Chuck Used in Plasma Processing

Gyu Il SHIM and Hideo SUGAI¹⁾

Department of Electrical Engineering and Computer Science, Nagoya University, Nagoya 464-8603, Japan

¹⁾*Department of Electronics and Information Engineering, Chubu University, Kasugai 487-8501, Japan*

(Received 17 June 2008 / Accepted 24 July 2008)

Comparative study on Coulomb type and Johnsen-Rahbek type of electrostatic chuck used for holding a silicon wafer in plasma processing is presented. The remarkable differences between the two types are found in dechuck operation where a high voltage applied to the chuck electrode is turned off to release the wafer from the chuck stage. In case of the Coulomb type, an instantaneous large short-circuit current flows exponentially decreasing with a short time constant ($\tau = 0.14$ ms). In case of the J-R type, a non-exponentially decaying small current is sustained for much longer time (~ 1000 ms), thus giving rise to the considerable delay of wafer dechuck. The mechanism of such decay is explained by a microscopic bi-layer model where the interfacial layer is divided into three distinct regions having their own capacitance and surface resistance.

© 2008 The Japan Society of Plasma Science and Nuclear Fusion Research

Keywords: electrostatic chuck, Johnsen-Rahbek effect, electrostatic dechuck, surface resistivity, bi-layer model

DOI: 10.1585/pfr.3.051

In many plasma process applications, electrostatic chuck (ESC) is used as a standard industrial tool for tightly chucking the object (silicon wafer) on a stage and dechucking it after processing. In a bipolar ESC configuration, a high voltage is split between the two plates embedded inside the chuck stage. On the other hand, a unipolar configuration is more commonly employed where a positive or negative high-voltage is applied between the chuck electrode molded in the ceramic stage and the grounded plasma vessel. Here the attractive Coulomb force yields between the electrode and the wafer by surface charges of opposite polarities just as in a two electrode capacitor. In the unipolar configuration, charging and discharging currents flow through plasma contacting the wafer. The wafer dechuck is done by switching off the high voltage in a presence of plasma, and after the charge extinction the wafer is lifted up by pins in the absence of plasma. In volume production of plasma-assisted semiconductor process, a number of silicon wafers are required to be speedily chucked and dechucked with use of a load-lock chamber.

Two types of ESC are conventionally employed in industry; Coulomb type [1–3] using insulating spacer layer (volume resistivity $\rho > 10^{14}$ Ω -cm), and Johnsen-Rahbek (J-R) type [4, 5] using semiconductive spacer layer ($\rho = 10^{10}$ – 10^{12} Ω -cm) between the plates (i.e., chuck electrode and wafer). In the J-R type, very strong holding force is achieved at lower chuck voltages than in the Coulomb type, owing to the J-R effect [6]: high electric fields appears at the metal-semiconductor interface with surface irregularities. Thus, the J-R type has an advantage of less arc-

ing troubles in high-voltage chuck operation while a large leakage current flowing in the chuck system may cause damages in the film on wafer. In dechuck operation, the wafer held by the Coulomb type ESC is easily detached after turning off the chuck voltage, however in case of the J-R type the electrostatic charges remain for a long time and wafer crack troubles some times occur during lift by pins for wafer replacement.

To avoid such troubles, a deeper understanding of the J-R type ESC is required, particularly on dechucking operation. Concerning the chuck operation of J-R type, we previously reported remarkable effects of RF-induced self-bias voltage [7] and a bi-layer equivalent circuit model [8] which successfully explained the behavior of the J-R chuck. In this paper, we focus on the dechuck operation, clearly demonstrating the difference between the Coulomb type and the J-R type.

The experiment was performed in an ICP device [9] where plasma is produced in a cylindrical stainless steel chamber, by 13.56 MHz RF discharge in argon at a typical pressure of 0.1 Torr. In order to compare the two types of ESC, we prepared the Coulomb chuck made of alumina (Al_2O_3 , $\rho \sim 5 \times 10^{16}$ Ω -cm) and the J-R chuck made of aluminum nitride (AlN, n-type semiconductor, $\rho \sim 2 \times 10^{10}$ Ω -cm). Both ESCs have the same geometrical sizes: the diameter of 200 mm, the thickness of 5 mm wherein the chuck electrode made of molybdenum is embedded with the separation $l = 0.54$ mm (spacer layer thickness) from the contacting wafer surface. The geometrical contact area of ESC is 60% of the projected area of chuck electrode, owing to a number of emboss (height

author's e-mail: sugai-h@isc.chubu.ac.jp

50 μm, area 2 × 2 mm²) prepared for helium gas cooling of wafer.

First of all, the Coulomb type ESC was installed with a 200-mm-diam silicon wafer in the ICP chamber. In the actual plasma processing, the chuck voltage is applied after plasma ignition where the wafer at the floating potential is electrically connected with the grounded chamber via plasma. In the present experiment, to make the problem simple and to avoid RF noise for small current measurements, the wafer was short-circuited to the ground by a metal wire in vacuum without plasma, and the voltage of $V_0 = 1$ kV was applied to the chuck electrode to hold the wafer. After then, the wafer was dechucked by switching off the applied voltage at the time $t = 0$, and the chuck current I was measured together with the chuck voltage V as shown in Fig. 1.

The semi-logarithmic plot in Fig. 1 indicates the exponential decay of I and V with the same time constant of $\tau = 0.14$ ms. This behavior is understood considering the equivalent circuit inserted in Fig. 1 (a). With the switch S_1 turned on and S_2 off, the chuck capacitance C is filled with charges, which are discharged in dechuck operation with S_1 off and S_2 on at the time $t = 0$, yielding the current $I(t)$ via the external resistance R_0 connected to the chuck voltage source. A simple circuit analysis gives the exponentially decaying current with the time constant $\tau = CR_0$ as

$$I(t) = (V_0/R_0) \exp(-t/\tau). \tag{1}$$

The measured current at $V_0 = 1$ kV in Fig. 1 (b) gives the initial value $V_0/R_0 = 40$ mA at $t = 0$, which leads to $R_0 = 25$ kΩ in accordance with the installed resistance $R_0 = 23$ kΩ. Furthermore, the measured time constant ($\tau = 0.14$ ms) allows us to estimate the capacitance to be $C = \tau/R_0 = 5.6$ nF. On the other hand, the calculation

from a well-known formula of parallel electrode capacitance gives slightly smaller value: $C = \epsilon_0 \epsilon_S S/l = 4.53$ nF for the specific dielectric constant of alumina $\epsilon_S = 8.8$, the area S of 200-mm-diam. wafer, and $l = 0.54$ mm. Using $C = 4.53$ nF, the initial charge Q_0 is estimated as $Q_0 = CV_0 = 4.53$ μC, along with the chuck holding force before dechuck to be $F_0 = (D^2/2\epsilon_0)S = 36.9$ N where the electric displacement $D = Q_0/S$. The estimated holding force agrees with the measured value $F_0 \sim 40$ N based on a helium gas pressurization method [8].

The remarkably different behaviors were found in dechuck operation of the J-R type as shown in Fig. 2. When the chuck voltage of $V_0 = 0.4$ kV is turned off at $t = 0$, a non-exponentially decreasing small current continues for long time (~1000 ms). It should be noted that the time scale of horizontal axis of Fig. 2 is three orders of magnitude larger compared with Fig. 1. The temporal variation of current I in Fig. 2 (b) can be fitted by superposing three exponentially decaying currents with different time constants $\tau_1 = 39$ ms, $\tau_2 = 260$ ms and $\tau_3 = 580$ ms as indicated by the dashed lines, although the measured slope dI/dt continuously and smoothly changes in time. On the other hand, as shown in Fig. 3, the careful measurement at the very early time $t < 0.5$ ms revealed a large current decreasing in the same time constant ($\tau_0 = 0.14$ ms) as the Coulomb type. It should be noted in this figure that the current starts to deviate from the exponential line at $t \sim 0.15$ ms and continues on the non-exponential curve in Fig. 2 (b). Thus, the current in the dechuck operation of the J-R type has four time constants ($\tau_0, \tau_1, \tau_2,$ and τ_3).

According to the charge conservation, the time integration of the current measured in Figs. 2 and 3 gives the steady state charge Q_0 stored in the J-R chuck at $t < 0$. Figure 4 shows the chuck charge Q_0 as a function of the

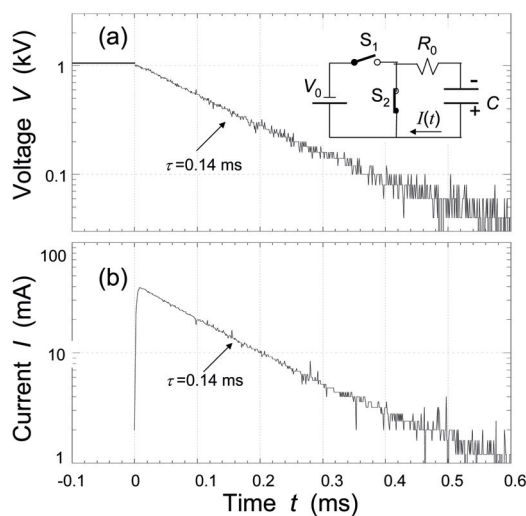


Fig. 1 (a) Chuck voltage V and (b) chuck current I in dechuck operation of Coulomb type ESC.

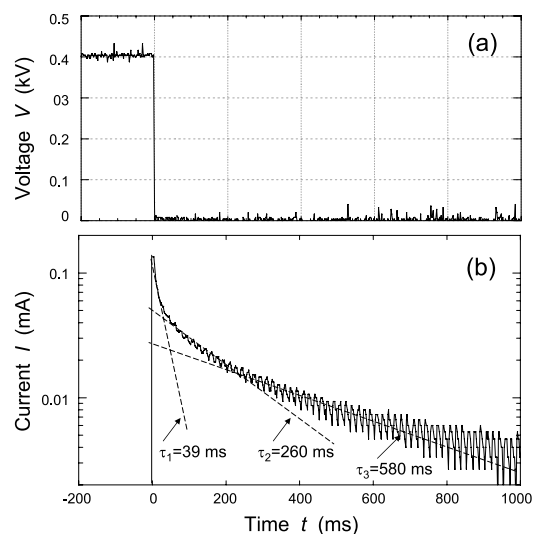


Fig. 2 (a) Chuck voltage V and (b) chuck current I in dechuck operation of J-R type ESC.

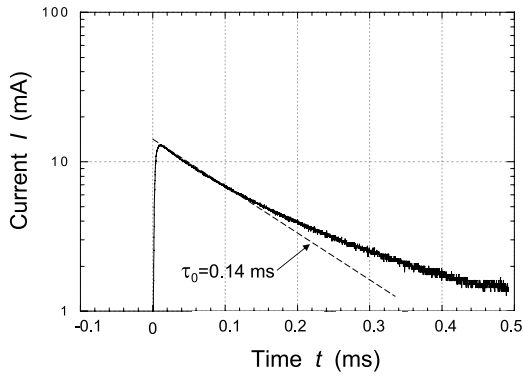


Fig. 3 Initial chuck current decay of J-R chuck.

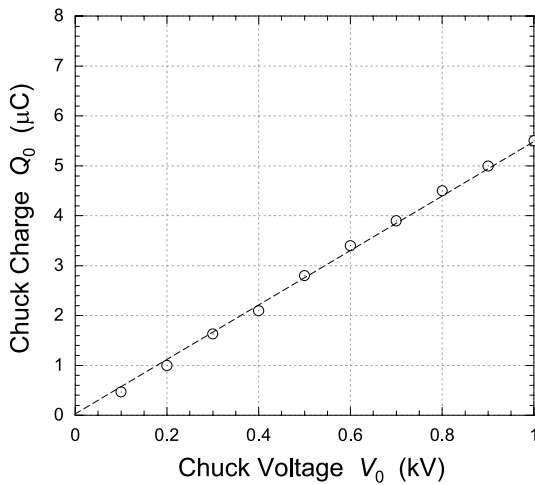


Fig. 4 The total charge Q_0 as a function of the voltage V_0 applied to J-R chuck.

applied chuck voltage V_0 obtained in this way. The slope of the dashed line in Fig. 4 gives the overall capacitance $C_0 = Q_0/V_0 = 5.7$ nF, which is in good agreement with the capacitance (5.6 nF) of the Coulomb type estimated from Fig. 1.

In order to understand such peculiar current decay, we consider the detailed structure of J-R chuck in the bi-layer model in Fig. 5, originally proposed in the previous paper [8]. With the switch S_1 closed and S_2 opened, the chuck voltage V_0 is applied between the wafer and the chuck electrode, and the current flows through a thick bulk layer into a thin interfacial layer of thickness δ . Let the x - and y -axis to be parallel and perpendicular to the wafer plane, respectively, and the origin ($x = y = 0$) to be at the bottom of hump which contacts the wafer around $x = w$.

The current flows uniformly along the y -axis in the bulk layer. In the interfacial layer, however, it concentrates toward the contact point area ($x \sim w, y = \delta$) as indicated by arrows in Fig. 5. Namely, the current path is bent near the boundary between the gap (ϵ_0) and the hump ($\epsilon_0 \epsilon_s$), and the current flows along a thin layer of the hump surface, thus causing the surface potential variation according

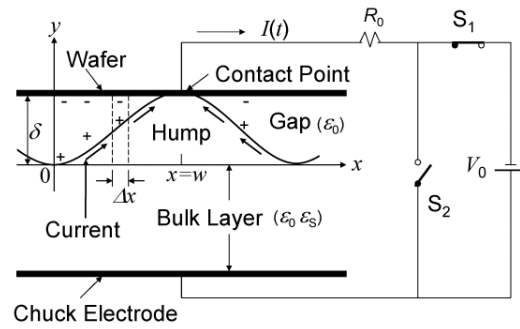


Fig. 5 Bi-layer model of J-R type ESC in chuck operation.

to the Ohm's law. In case where the bulk layer resistance should be negligible, the voltage V_0 will be applied directly to the origin ($x = y = 0$), and the surface potential gradually decreases along the current path. Thus, the gap between the wafer and the hump surface can be regarded as distributed vacuum condensers: the capacitance between x and $x + \Delta x$ can be expressed as $\Delta C(x) = \epsilon_0 \Delta S / \gamma$ for the surface area ΔS and the gap length γ . The charge is given by the local voltage $V(x)$ as $\Delta Q(x) = V(x) \Delta C(x)$. This surface charge generates the electric field normal to the hump surface which in turn bends the original electric field E_y along the y -axis, thus making the overall electric field parallel to the hump surface. The surface resistance is determined by the thickness and the length of current channel, the volume resistivity ρ , and the defect density in surface layer. In actual J-R chucks, numerous humps contact the wafer with various gap length δ and hump size w .

In the dechuck operation, the switch S_1 is opened with S_2 closed, and the stored charges are short-circuited by the current flowing in the opposite direction through the resistances along the hump surface and the bulk layer. As described above, the capacitance is continuously distributed inside the gap, and hence the total interfacial capacitance C_1 can be expressed by surface integral over the interfacial surface S as

$$C_1 = \int_S C(x) dS = \int_S \epsilon_0 \delta(x)^{-1} dS, \quad (2)$$

where $\delta(x)$ is the gap length. Here it should be noted in Fig. 2 (b) that the chuck current can be approximated by superposing *three* exponential functions with different time constants, suggesting different capacitances. With this result, the interfacial layer capacitance is simply divided into *three* capacitances, depending on the distance from the contact point, as illustrated in Fig. 6. The first capacitance C_1 is allotted to the contacting region around $x = w$, the second capacitance C_2 is assigned to the mid-range, and the third capacitance C_3 is allotted to the bottom region around $x = 0$. The charge stored in each capacitance C_n ($n = 1, 2, 3$) is carried by the current I_n through the surface resistance R_{S_n} and the bulk resistance R_{B_n} as shown in the equivalent circuit in Fig. 6 (b). Here the impedance

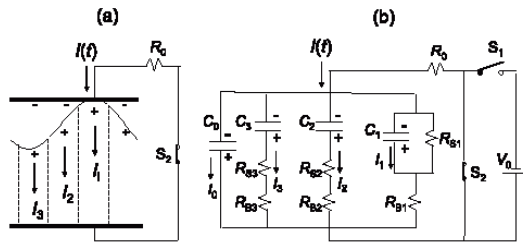


Fig. 6 Modified equivalent circuit model of J-R chuck in dechuck operation.

of the contact region is expressed as the parallel connection of C_1 and R_{S1} as a result of the J-R effect where the metal-semiconductor contact gives rise to a surface potential barrier (Schottky barrier) and a thick depletion layer of carrier conduction. As seen in Fig. 6 (a), the current loop of I_3 passes through the contact layer, the surface layer of hump, and the bulk layer (R_{B3}). The value of R_{S3} in the circuit Fig. 6 (b) includes the contact layer resistance R_{S1} and the hump surface resistance R_{S2} . Similarly, the value of R_{S2} includes the contact layer resistance R_{S1} .

Here we denote the initial values of voltage, current, and charge of each capacitance C_n to be V_{n0} , I_{n0} , and q_n at $t = 0$, along with the resistance $R_n = R_{S_n} + R_{B_n}$. Neglecting the small external resistance R_0 (23 kΩ in the present experiment), we find the time variation of each current $I_n(t)$ for $t > 0$ as

$$I_n(t) = I_{n0} \exp(-t/\tau_n), \tag{3}$$

where $I_{n0} = V_{n0}/R_n$ and the time constant $\tau_n = C_n R_n$. The integration of $I_n(t)$ from $t = 0$ to infinity gives the charge $q_n = \tau_n I_{n0}$.

In addition to the interfacial capacitances, the bulk layer capacitance $C_0 = \epsilon_0 \epsilon_S S/l$ is introduced in Fig. 6 (b) which gives the current $I_0(t) = I_{00} \exp(-t/\tau_0)$ flowing through the external resistance R_0 without passing the bulk and interfacial layers. The measured current in Fig. 2 corresponds to the total current ($I_0 + I_1 + I_2 + I_3$), the time integration of which gives the total charge Q_0 shown in

Fig. 4. For example, at the chuck voltage $V_0 = 0.4$ kV, the measured value is $Q_0 = 2.1 \mu\text{C}$, which is larger than the charge $q_0 = \tau_0 I_{00} = 1.82 \mu\text{C}$ calculated from the integration of $I_0(t)$ for the measured values of $\tau_0 = 0.14$ ms and $I_{00} = 13$ mA. The difference of $(Q_0 - q_0) = 0.28 \mu\text{C}$ is considered to be stored in the interfacial capacitances (C_1 , C_2 , and C_3). Thus, the interfacial charges are small compared with the bulk charge, however the large attractive force arises owing to the gap distance much smaller than the bulk layer thickness ($l = 0.54$ mm).

In conclusion, dechuck operation of Coulomb type and Johnsen-Rahbek type ESC in unipolar configuration was investigated. After switching off the high voltage, the charge stored in the Coulomb chuck is rapidly extinct through an exponentially decaying current with a short time constant ($\tau = 0.14$ ms) which is given by the chuck capacitance C and the internal resistance R_0 of voltage source. Thus, the dechuck delay time and the initial dechuck current of the Coulomb type can be controlled by adjusting the values of C and R_0 . In case of the J-R chuck, the stored charge survives for much longer time (~ 1000 ms), thus making the wafer dechuck difficult. Such complex behavior of the J-R chuck is described by the microscopic bi-layer model introducing three distinct regions in the interfacial layer. The dechuck delay time of the J-R chuck may be shortened by increasing the gap length (surface roughness) and by reducing the volume resistivity of insulating spacer layer, considering the trade-off with suppression of the current-induced damage and power reduction of the DC high voltage source.

- [1] G.A. Wardly, Rev. Sci. Instrum. **44**, 1506 (1973).
- [2] J.P. Scott, Solid State Technol. **20**, 43 (1997).
- [3] R. Ward, J. Vac. Sci. Technol. **16**, 1830 (1979).
- [4] J. Field, Solid State Technol. **17**, 91 (1994).
- [5] L.D. Hartssough, Solid State Technol. **16**, 87 (1993).
- [6] F.A. Johnsen and K. Rahbek, J. Inst. Elect. Engrs. **61**, 713 (1923).
- [7] G.I. Shim and H. Sugai, Plasma Fusion Res. **2**, 044 (2007).
- [8] G.I. Shim and H. Sugai, Plasma Fusion Res. **3**, 028 (2008).
- [9] G.I. Shim and H. Sugai, Proc. 6th Int. Sympo. Dry Process, Nagoya, 77 (2006).